Enhanced removal of 2,4-dichlorophenol by coupling of Pd nanoparticles with biofilm

Chengyang Wu, Jingzhou Zhou, Si Pang, Lin Yang, Xiaodi Li, Eric Lichtfouse, Siqing Xia, Hongbo Liu

Journal of Environmental Chemical Engineering 12 (2024) 112176

https://doi.org/10.1016/j.jece.2024.112176

Enhanced removal of 2,4-dichlorophenol by coupling of Pd nanoparticles with biofilm

Chengyang Wu [a], Jingzhou Zhou [b], Si Pang [b], Lin Yang [b], Xiaodi Li [b], Eric Lichtfouse [c], Siqing Xia [b], Hongbo Liu [a,*]

[a] School of Environment and Architecture, University of Shanghai for Science and Technology, 516 Jungong Road, Shanghai, China
[b] State Key Laboratory of Pollution Control and Resource Reuse, College of Environmental Science and Engineering, Tongji University, 1239 Siping Road, Shanghai, China
[c] State Key Laboratory of Multiphase Flow in Power Engineering, Xi'an Jiaotong University, 28 Xianning West Rd, Xi'an, Shaanxi 710049, China

ARTICLE INFO

Editor: Yujie Men

Keywords:
2,4-dichlorophenol
Palladium nanoparticle
Biofilm
Reductive dechlorination

ABSTRACT

The persistence of chlorinated phenols in the environment is a major concern due to their persistence and toxicity, yet advanced remediation methods are actually limited. For instance, reductive dechlorination of chlorophenols utilizing palladium nanoparticles (PdNPs) supported on hydrogen-transfer membranes is not fully efficient. Here we tested the simultaneous microbial-driven and Pd-catalyzed reduction of 2,4-dichlorophenol (2,4-DCP) for removal rate, selectivity of reduction products, and optimal reaction conditions. For that we compared three hydrogen-based membrane reactors: a 'Pd-biofilm reactor' with Pd nanoparticles and a biofilm, with two controls: a 'biofilm reactor' with biofilm alone, and a 'Pd-film reactor' with Pd nanoparticles alone. Results show that the Pd-biofilm reactor removed 89.3% of total phenols, versus 15.7% for the biofilm reactor and 19.5% for the Pd-film reactor. The strong adsorption capacity of Pd-biofilm enhanced dechlorination. This elevated local chlorophenols concentration led to a 2–4 times higher reduction rate within Pd-biofilm compared to abiotic Pd-film. The presence of nitrate enhances phenol removal over Pd-biofilm but inhibited 2,4-DCP dechlorination. Similarly, high concentrations of nitrite, above 250 μM, inhibited 2,4-DCP reduction, predominantly in microbial processes rather than in catalytic reduction. Increasing hydrogen pressure facilitated the reduction of both 2,4-DCP and nitrate by Pd-biofilm, with an optimal pH of 7.0 for Pd-biofilm. The Pd-biofilm reactor decreased total phenols from 5–10 mg L^{-1} to the recommended threshold of 0.1 mg L^{-1} in 55 days, thus appearing as an efficient technique to clean chlorophenol-contaminated waters.

1. Introduction

With large usage in production of preservatives and herbicides, 2,4-dichlorophenol (2,4-DCP) is emerging as one of the most prevalent chlorophenols found in aquatic environments. 2,4-DCP has been detected at ppm levels in raw water [10] and is classified as a priority pollutant by the United States Environmental Protection Agency (EPA) (2012) due to its carcinogenicity, cytotoxicity, and slow biodegradation. The maximum contaminant level for 2,4-DCP in drinking water is set at 0.1 mg L^{-1} by the EPA.

The strong carbon-chlorine bond (~ 400 kJ $mole^{-1}$) (Luo and Yu-Ran, 2007) renders chlorinated phenols resistant to biological degradation under ambient conditions [14]. Conventional destructive methods, such as advanced oxidation [22], electrochemical processes [18], and photocatalytic degradation [8], demand significant energy inputs. Nondestructive removal methods, including adsorption, ion exchange, liquid-liquid extraction, are considered less environmentally friendly due to their tendency to produce harmful byproducts [9]. Catalytic hydrodechlorination (HDC) using platinum group catalysts offers a promising approach for dechlorination, because it only requires hydrogen gas (H_2) as the chemical input and provides fast kinetics, mild operating conditions, and no secondary waste stream. Among the catalysts, palladium (Pd) is the most studied catalyst due to its great H_2-absorption capacity and ability to form highly reductive atomic hydrogen on the catalyst's surface, which is activated to substitute the Cl atoms in chlorophenols. However, Pd-based reductive dechlorination by conventional catalytic approaches have encountered challenges: poor efficiency of the H_2 supply and catalyst deactivation due to its loss.

A palladized membrane biofilm reactor (Pd-MBfR) tackles the challenges of low efficiency in H_2 supply and maintaining long-lifespan

* Corresponding author.
E-mail address: Liuhb@usst.edu.cn (H. Liu).

stability of catalysts [24]. The Pd-MBfR enables complete H_2 utilization and the formation of a robust Pd-catalyst by efficient bubble-free delivery of H_2 through nonporous membrane fibers, which is precisely controlled by the H_2 pressure. The Pd-MBfR also facilitates microbially driven Pd recovery to form palladium nanoparticles (PdNPs) associate with the biofilm (Pd-biofilm), thereby efficiently immobilizing and stabilizing them to enhance hydrodechlorination.

Nitrate often accompanies 2,4-DCP as a common co-contaminant in water [31]. The reduction of nitrate over the Pd-biofilm can have dual effects—stimulating the mineralization of dechlorination product phenol on one hand, and competitively inhibiting catalytic dechlorination on the other [24]. Moreover, factors such as the influent surface loading, pH, and electron donor supplying flux can influence the dechlorination performance of chlorinated solvents and the selectivity of the products [16]. However, the effect of these factors on the synergistic 2,4-DCP removal within the Pd-MBfR remains unexplored.

In a recent study, we developed a Pd-MBfR by coupling a biofilm with in-situ generated PdNPs and documented that the Pd-MBfR facilitated hydrodechlorination and mineralization of 2,4-DCP [24]. We proposed distinct pathways for 2,4-DCP dechlorination on PdNP surfaces, followed by microbial mineralization via denitrification. Due to the lack of optimized operational conditions for the Pd-MBfR, the dechlorination performance needs improvement. Here, we conducted a comprehensive characterization of the removal performances for 2, 4-DCP and its intermediate products in three membrane reactor systems. We compared biofilm-only, PdNP-only, and Pd-biofilm setups under varying surface loadings of 2,4-DCP over approximately 55 days of continuous operation. To identify the optimal operational conditions for 2,4-DCP removal by the Pd-MBfR, we also investigated the effect of 2,4-DCP loading, nitrate loading, nitrite loading, H_2 pressure, and pH on 2,4-DCP removal. The aim of this study is to discover the mechanisms underlying the improved removal performance of phenols and shed light on the potential benefits of the synergetic platform.

2. Materials and methods

2.1. Configuration and setup of the reactors

Experiments were carried out with three reactors in parallel, which were similar to that used in a previous study (Fig. S1, Supporting Information) [26]. Each reactor consisted of two interconnected tubes via Viton tubing (Saint-Gobain, USA), one containing a bundle of 32 nonporous polypropylene hollow-fiber membranes (Teijin, Japan) with both ends connected to the H_2 gas pipeline, while the other contained a coupon bundle of 10 identical fibers, with upper end connected to the pipeline. With a working volume of 65 mL and a total membrane surface area of 54 cm^2. The liquid in the reactor was well mixed by a recirculation rate of 150 mL min^{-1} provided by a peristaltic pump (Longer, China). Throughout the experiments, the temperature was consistently maintained at 25 ± 2 °C.

2.2. Inoculation, feeding, and startup of the membrane biofilm reactors

We inoculated two of the three reactors ("MBfR" and "Pd-MBfR") with anoxic sludge from Wusong wastewater treatment plant (Shanghai, China) and fed the reactors continuously with a 0.7-mM NO_3^- medium to accumulate biofilms on the membranes. The components of the foundational medium are summarized in supplementary Table S1. After two months, mature biofilms had successfully developed on the membrane fibers. The specifics of the inoculation and feeding procedures were described in a previous study [24].

2.3. Synthesis and retention of Pd nanoparticles on membrane surfaces

We introduced Pd(II) medium (160 mg L^{-1} Pd(II) as Na_2PdCl_4) into one of the MBfRs and a parallel non-inoculated reactor, operating in batch mode under an H_2 pressure of 15 psig (2.0 atm, absolute pressure) to produce PdNPs within the biofilm (Pd-biofilm) and on the surface of membranes (Pd-film), respectively. The composition of the Pd(II)-containing medium is detailed in a previous study [25]. The Pd (0)-deposition process lasted for 48 h until dark precipitates were observed on the fiber bundles of both reactors, and more than 99% of the input Pd(II) was recovered after each addition. A total of 31 mg of Pd was retained, either through direct deposition onto the fiber surfaces in the Pd-film (establishing the membrane Pd-film reactor) or through association with the biofilm in the Pd-biofilm (establishing the Pd-MBfR).

2.4. Continuous operation for 2,4-dichlorophenol removal

During Stage I (Day 1–12), the reactors were fed with the medium containing 360 μM NO_3^- and 30.7 μM 2,4-DCP. In Stage II (Day 13–35), the influent medium was modified to include 61.3 μM of 2,4-DCP. In Stage III, the applied H_2 pressure was increased from 7 psig to 15 psig. Specific operational parameters for each stage are summarized in Table 1. Steady-state conditions were reached in each stage when the effluent concentrations of chlorophenols and NO_3^- remained stable for at least 3 days with a variation of less than 10%. The influent medium was degassed with N_2 for 15 min before use, resulting in a dissolved oxygen (DO) concentration in the influent medium of less than 0.15 mg L^{-1}. 5-mM 2,4-DCP stock solutions were prepared by dissolving them in deoxygenated water and stored at 4 ℃, which were added into influent water during the experiments. 2-mM phosphate buffer was added to the influent, and the pH values of the influent were maintained within the range of 7.2 ± 0.2.

2.5. Optimal conditions for 2,4-DCP removal

After operating the three reactors for 55 days, short-term experiments were conducted to investigate how 2,4-DCP loading, NO_3^- loading, NO_2^- loading, H_2 availability, and pH affected 2,4-DCP removal systematically. The experiments were organized into five series (Table S2), with hydraulic retention time (HRT) maintained at 4.5 h. Prior to each test, the three reactors were returned to the steady-state condition with an influent of 100 μM 2,4-DCP, 85 μM NO_3^-, 15 psig H_2 pressure, and pH 7.0. For each short-term test, the change of system conditions lasted for 5 HRTs to reach steady state, before samples were taken. Replicate samples were collected at 6, 7, and 8 HRTs and the results are presented as the average values.

2.6. Analytical methods

The liquid samples in the three reactors were collected using 10-mL syringes and filtered through 0.22-μm PTFE membrane filters. The concentrations of Pd(II) was determined using inductively coupled plasma-mass spectrometry (ICP-MS, Agilent 7700, Agilent Technologies, USA). For the analysis of 2,4-DCP, ortho-chlorophenol (2-CP), para-chlorophenol (4-CP), and phenol, the filtered samples were subjected to high-performance liquid chromatography with an Agilent C18 column (HPLC, Shimadzu LC-20A, Japan). NO_3^- and NO_2^- were analyzed by an ion chromatograph (IC, Dionex Aquion, USA) with an AS-19 column. pH and DO were measured using a multi-Parameter Meter (HACH HQ40d, USA).

2.7. Characterization of solid state

At the end of Stage III, solid samples from the three reactors were collected by excising fiber segments approximately 5 cm in length from the coupon fibers, and the remaining fiber was sealed by tying the end into a knot. After chemical fixation and ultra-microtome slicing, these fiber sections were characterized by transmission electron microscopy (FEI Tecnai G2 F20, USA) equipped with energy-dispersive X-ray

Table 1
Parameters for operations and average performance for each stage of the palladized membrane biofilm reactor (Pd-MBfR), membrane biofilm reactor (MBfR), and membrane palladium-film rector (Pd-film reactor) at steady state.

stage	days	H_2 pressure psig	HRT	2,4-DCP							
				in μM	surface loading mmol m^{-2} d^{-1}	out μM			total phenols removal %		
						Pd-MBfR	MBfR	Pd-film reactor	Pd-MBfR	MBfR	Pd-film reactor
Stage I	0-12	7	4.5 h	30.7	2.1	9.1	24.7	8.2	63.4	16.7	19.0
Stage II	13-35	15		61.3	4.1	10.7	14.2	9.6	77.5	11.8	18.8
Stage III	36-55	15		61.3	4.1	2.5	6.1	5.6	89.3	15.7	19.5

spectroscopy (EDX). Solid was scraped from the fibers in the rectors and then freeze-dried them for subsequent X-ray diffraction (XRD) using an X' Pert PRO MPD diffractometer with Cu- Kα radiation. Detailed protocols for sample fixation and slicing, as well as instrument specifications, can be found in previously published studies [24,27].

2.8. Analysis of microbial communities

At the end of Stage III, a 10-cm section was excised from a coupon fiber in the Pd-MBfR or MBfR. We followed the procedures of biofilm separation and DNA extraction described by Xia et al. [29]. After amplifying and purifying, the bacterial 16 S rRNA gene were sent to Majorbio Technology (Shanghai, China) for processing Illumina MiSeq sequencing, conducted in accordance with established protocols.

2.9. Fluxes calculations

The fluxes of the substrates (J) were calculated by

$$J = \frac{Q(C_0 - C_e)}{A} \quad (1)$$

where J is the flux, mmol m^{-2} d^{-1}; Q is the influent flow rate, m^3 d^{-1}; C_0 and C_e are influent and effluent concentrations of each substrate (chlorophenols and NO_3^-), mmol m^{-3}; and A is the effective membrane surface area, m^2. The dechlorination flux in electron equivalents (e^--meq m^{-2} d^{-1}) was calculated based on released Cl^- concentrations according to reaction stoichiometry:

$$2,4-\mathrm{DCP} + 4e^- + 2H^+ \rightarrow \mathrm{phenol} + 2Cl^- \quad (2)$$

The NO_3^- flux in electron equivalents (e^--meq m^{-2} d^{-1}) was calculated from Eqs. (3)–(5):

$$NO_3^- + 5e^- + 6H^+ \rightarrow 0.5N_2 + 3H_2O \quad (3)$$

$$NO_3^- + 2e^- + 2H^+ \rightarrow NO_2^- + H_2O \quad (4)$$

$$NO_3^- + 8e^- + 10H^+ \rightarrow NH_4^+ + 3H_2O \quad (5)$$

To indicate if the H_2 supply was limiting, the maximum H_2-supply flux at applied H_2 pressure of 15 psig (i.e., 300 e^--meq m^{-2} d^{-1}) was calculated according to Tang et al. [19].

3. Results and discussion

3.1. Characterization of the membrane-supported Pd-biofilm, Pd-film, and biofilm

Dried powder samples were collected from the coupon bundle in the Pd-MBfR and the Pd-film reactor for TEM, and XRD analyses. Fig. 1a

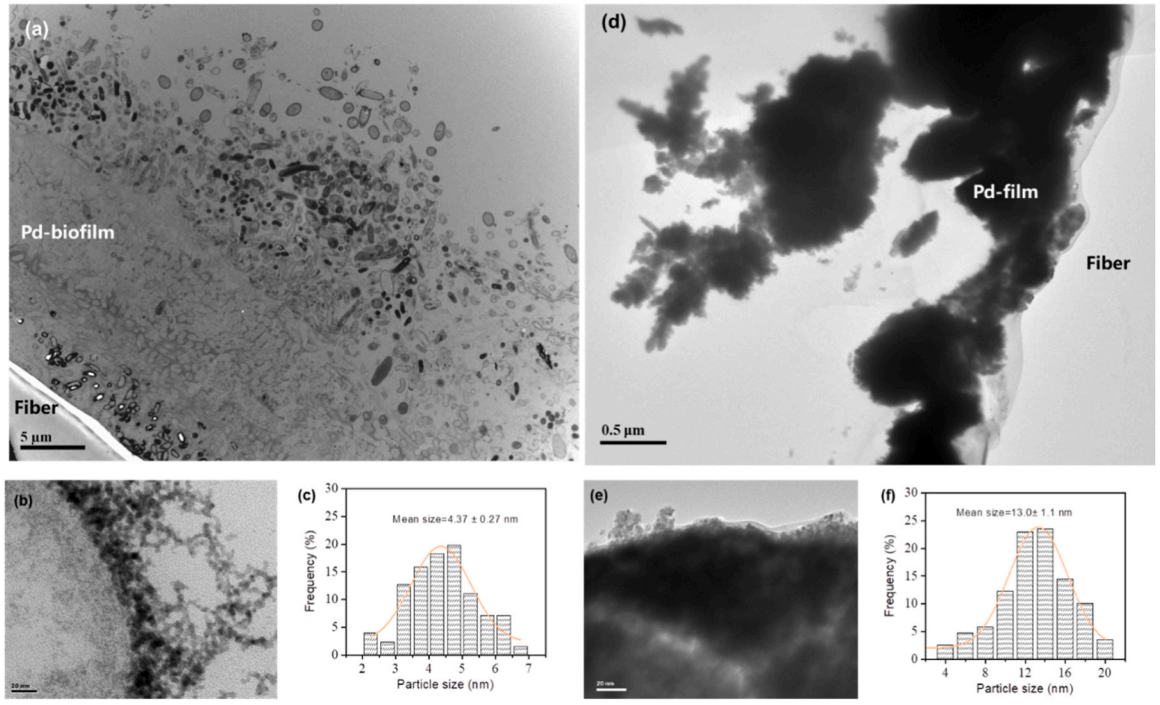

Fig. 1. Transmission electron microscopy (TEM) images of selected areas in cross sections of Pd-biofilm (a) and Pd-film (d). The grey shapes are bacterial cells, and the dark spots are Pd(0). High resolution transmission electron microscopy (HRTEM) images of Pd(0) crystallites in Pd-biofilm (b) and Pd-film (e). Size distribution histograms of the Pd nanoparticles on the edge of the aggregated Pd-film (c) and deposited on the microbial cell surface of Pd-biofilm (f).

presents the thickness of the Pd-biofilm attached to the hollow fiber was approximately 40 μm. The microbial cells exhibit elliptical or circular shapes, with a denser arrangement closer to one side of the fiber (within 20 μm distance from the fiber surface). Fig. 1b demonstrates that black PdNPs were mainly distributed on the surface of microbial cells and within the extracellular polymeric substances (EPS), with a small portion present inside the microbial cells. The particle size distribution of the PdNPs in Fig. 1c reveals that the average size is approximately 4.37 ± 0.27 nm. Compared to the Pd-biofilm sample, the thickness of the PdNPs-film attached to the outer surface of the fiber was approximately 1.75 μm (Fig. 1d), and the majority of PdNPs were aggregated near the fiber. The statistic average size of PdNPs is approximately 13.0 ± 1.1 nm (Fig. 1f), indicating mild aggregation and clustering of Pd(0) deposits due to insufficient stabilization [34]. The XRD spectra of freeze-dried sample collected from the fibers (Fig. S2 in Supporting Information) exhibited four distinct diffraction peaks at 2θ angles of 40.1° (1 1 1), 46.7° (2 0 0), 68.1° (2 2 0), and 82.1° (3 1 1) in the XRD spectra, confirming the predominant presence of the Pd(0) crystal structure with dominant facets of (1 1 1) in both reactors.

3.2. Continuous dechlorination and mineralization of 2,4-dichlorophenol

After feeding the Pd-MBfR with the medium containing 30.7 μM of 2,4-DCP, intermediate products were undetected in the effluent during the first two days (Fig. 2a). Then, phenol started to accumulate in the effluent, along with the appearance of 2-CP on day 3. Increasing the influent concentration of 2,4-DCP to 61.3 μM resulted in in a subsequent phenol accumulation, reaching a maximum concentration of 20.6 μM (Stage II). After day 20, Pd-MBfR achieved stable removal for both 2,4-DCP and the intermediate products. To further improve the removal rate, the hydrogen pressure was increased to 15 psig (1.0 atm) (Stage III). In Stage III, the effluent concentrations of 2,4-DCP, 2-CP, and phenol were approximately 1.8 μM, 1.0 μM, and 3.6 μM, respectively, resulting in a total phenols removal of approximately 89.3%. These results demonstrate that Pd-MBfR exhibited complete removal of 2,4-DCP with minimal phenolic intermediates.

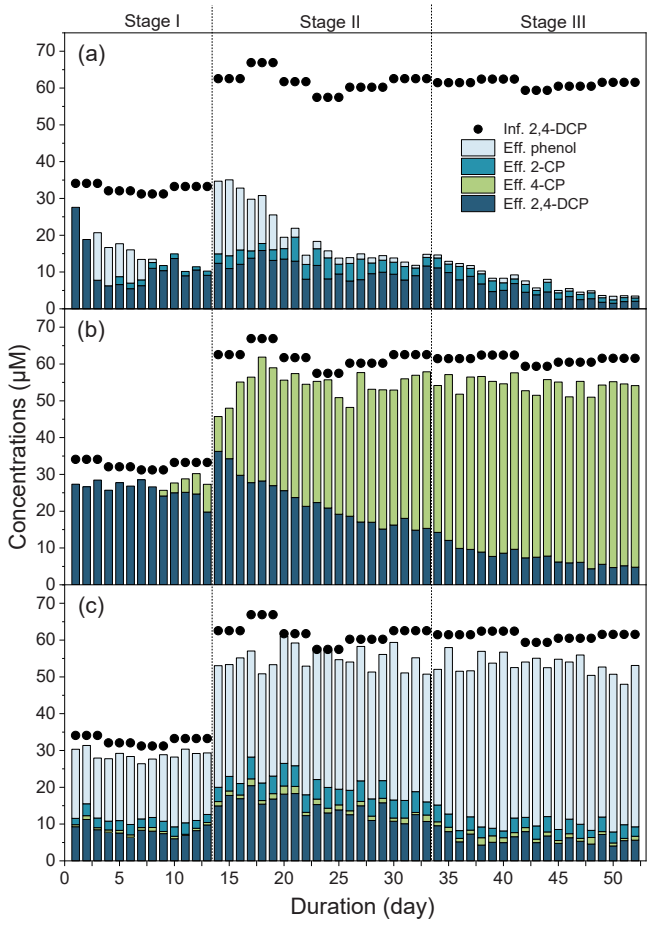

Fig. 2. The variation in influent and effluent concentrations of 2,4-DCP during the reduction stage for the palladized membrane biofilm reactor (Pd-MBfR) (a), membrane biofilm reactor (MBfR) (b), and membrane palladium-film rector (Pd-film reactor) (c). 2,4-DCP, 2-CP, 4-CP denotes 2,4-dichlorophenol, ortho-chlorophenol, and para-chlorophenol, respectively.

Parallel operation of the MBfR and the Pd-film reactor was conducted to compare their performance in 2,4-DCP removal and to understand the advantages of the Pd-MBfR. In the MBfR, the intermediate product, 4-CP, generated from the reduction of 2,4-DCP was apparently accumulated (Fig. 2b). The concentration of 2,4-DCP in the effluent continued to decrease and eventually stabilized around 4.91 μM in Stage III, resulting in a 2,4-DCP removal of 92.0%, which was comparable to that achieved by the Pd-MBfR. However, the significant accumulation of 4-CP led to a total removal of phenols of merely 15.7%. These results demonstrate that the MBfR exhibited efficient removal for 2,4-DCP, but the removal of intermediate 4-CP is deficient, leading to 4-CP accumulation and the low removal rate of total phenols.

As shown in Fig. 2c, the intermediate products of 2-CP, 4-CP, and phenol were detected in the Pd-film reactor effluent. The 2,4-DCP removal achieved by the Pd-film reactor was 93.4%, which is lower than the average removal rate of the Pd-MBfR (96.0%). Moreover, a significant accumulation of phenol led to a total removal of phenols of less than 20%. When the influent concentration of 2,4-DCP doubled in Stage III, the concentrations of all phenolic products in the effluent increased accordingly, and their proportions remained almost unchanged. The ratio of 2,4-DCP, 4-CP, 2-CP, and phenol in the effluent was 28.3%, 2.3%, 9.3%, and 60.4%, respectively. The H_2 supplying flux had a distinct impact on the reduction of 2,4-DCP in the Pd-film reactor. When H_2 pressure was doubled in Stage III, the ratio of 2,4-DCP, 4-CP, 2-CP, and phenol in the effluent changed to 10.4%, 2.0%, 6.3%, and 81.3%, respectively. These results demonstrate that the Pd-film reactor exhibited strong reduction potential for 2,4-DCP but had a limitation in removal of the dechlorination product, phenol.

In summary, the MBfR struggled to reduce 4-CP, while the Pd-film reactor faced challenges in phenol removal. The Pd-MBfR demonstrated the effective overall removal of 2,4-DCP and its intermediate products. The complete removal of 2,4-DCP by Pd-MBfR is the result of a synergy between catalytic dechlorination and microbial mineralization. The Pd-MBfR efficiently hydrodechlorinated 2,4-DCP to phenol, which was utilized as a more favorable electron donor than H_2 for denitrification and was mineralized to CO_2 [24].

Fig. 3 illustrates the microbial communities of biofilms in the Pd-

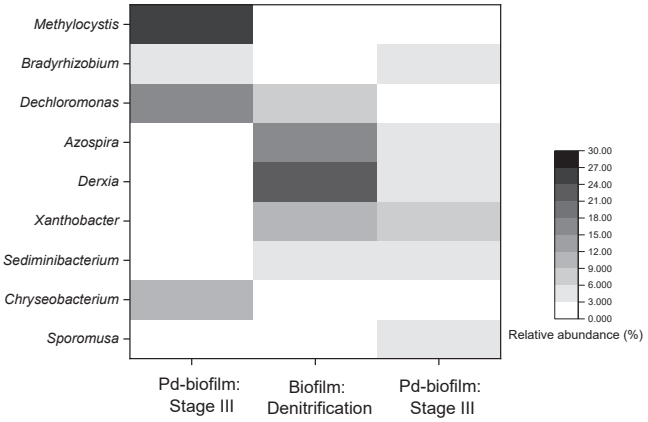

Fig. 3. Phylogenetic profiling of the Pd-biofilm and biofilm at the genus levels, < 3% phylotypes in the biofilms are not shown.

MBfR and MBfR at the genus level. In Stage III of the Pd-MBfR, *Methylocystis*, *Dechloromonas*, *Chryseobacterium*, and *Bradyrhizobium* are the dominant genera, with relative abundances of 25.1%, 15.3%, 11.9%, and 5.7%, respectively. *Methylocystis* belongs to type II methanotrophic bacteria [23] and can release soluble organic compounds as electron donors for denitrifying bacteria during methane oxidation [17]. Studies have also shown that *Chryseobacterium* can efficiently degrade methane [33]. The increase in the relative abundances of these two bacteria indicates the production of a significant amount of methane through the monooxygenation pathway [13] during the reduction of 2,4-DCP in the Pd-MBfR, which was observed in our previous study [24]. *Dechloromonas* is a common denitrifying bacterium that can degrade benzene under anaerobic conditions, with phenol being an intermediate in the degradation process [6,7]. *Bradyrhizobium* is a denitrifying bacterium [1].

3.3. Effects of typical conditions on dechlorination

3.3.1. Optimal 2,4-dichlorophenol loading effectuated full dechlorination in the Pd-MBfR

We conducted separate batch tests to investigate the kinetics of 2,4-DCP reduction in the three reactors. The influent concentrations used in these tests were 25, 45, 70, 100, and 140 μM, respectively (Table S2). The supply of electron donors was sufficient, as the dechlorination fluxes were significantly lower than the maximum H_2 flux (300 e^--meq m^{-2} d^{-1}). For the three reactors (Fig. 4a), the effluent concentrations of 2,4-DCP and its intermediate products (2-CP, 4-CP, and phenol) increased with higher influent concentrations of 2,4-DCP, and the electron equivalents flux consumed by dechlorination also increased with higher influent concentrations. Conversely, the removal showed an inverse relationship with the influent concentrations. In the Pd-MBfR, as the influent concentration increased from 45 μM to 70 μM, the removal of 2,4-DCP dropped abruptly from 97.6% to 90.2%. Similarly, in the MBfR (Fig. 4c), the influent concentration increased from 45 μM to 70 μM resulted in a sharp drop in 2,4-DCP removal rate from 88.7% to 77.4%. In the Pd-film reactor (Fig. 4e), the effluent concentrations of 2,4-DCP and its intermediate products increased with higher influent concentrations of 2,4-DCP, and the removal rate remained relatively stable at around 91.9%. It became apparent that when treating influent concentrations below 70 μM (surface loading of 2,4-DCP was < 4.7 mmol m^{-2} d^{-1}), the Pd-MBfR exhibited the highest removal rate for 2,4-DCP and total phenols. The 2,4-DCP-adsorption capacity of Pd-biofilm was reported to be 2- to 5-fold greater than that of abiotic Pd-film [25]. This enhanced adsorption had the effect of accelerating dechlorination by Pd-biofilm, especially its selectivity towards phenol rather than mono-chlorophenols. The Pd-MBfR gave a greater reduction rate than that did the Pd-film reactor, particularly for lower 2,4-DCP loadings, because adsorption of 2,4-DCP by the biofilm enhanced the catalytic contact of 2,4-DCP with activated hydrogen on Pd surface.

To estimate the reaction order, log J versus log C (Rittmann and McCarty, 2020) is plotted in the Fig. S3, and the results of reaction kinetics parameters for 2,4-DCP reduction are presented in Table 2. The reaction order for 2,4-DCP reduction in the MBfR was 0.52, which is close to the well-known half-order kinetics that was for deep biofilms in which the reaction is zero order in substrate concentration (Rittmann and McCarty, 2020). Chung et al. reported comparable findings in their research on the reduction of selenate and chromate using an MBfR [3,4], where the reaction orders in the biofilm were 0.41 and 0.49, respectively. When the reaction order is less than 1, the increase in the removal flux of 2,4-DCP is smaller than the increase in influent concentration, which resulted in a decrease in the removal rate. In the Pd-MBfR, the reaction order for 2,4-DCP reduction (0.48) indicates half-order kinetics. The Pd-MBfR exhibited a higher removal rate of 2,4-DCP compared to the MBfR, since the reaction constant approximately twice as large. This suggests that the reduction of 2,4-DCP in the Pd-MBfR primarily driven by the catalytic reduction over PdNPs distributed within EPS. Due to the

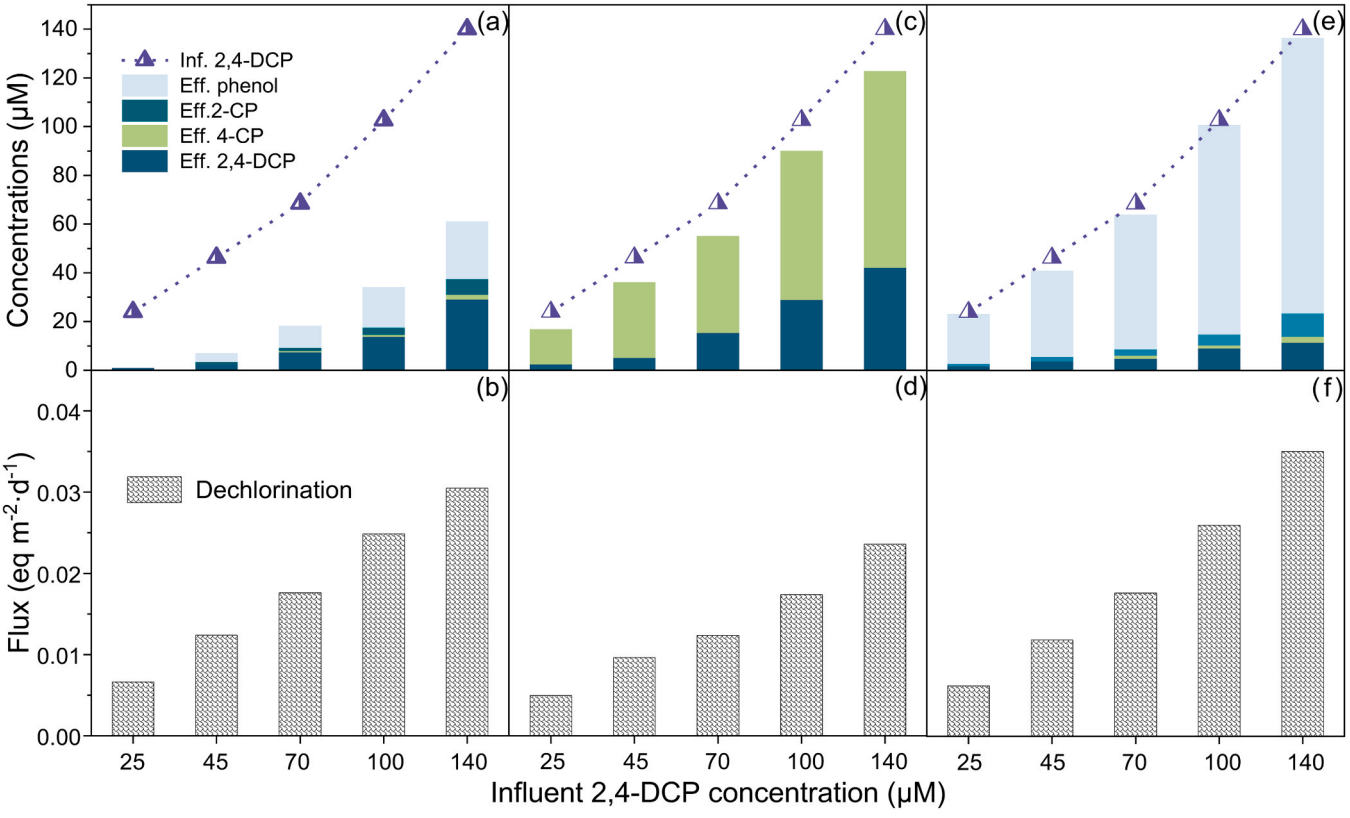

Fig. 4. The effect of influent 2,4-dichlorophenol loading on 2,4-dichlorophenol reduction in the Pd-biofilm reactor (a, b), the biofilm reactor (c, d), and the Pd-film reactor (e, f).

Table 2
Parameters of reduction kinetics in steady state under various influent concentrations of 2,4-dichlorophenol.

Reactors	Effluent concentration (μM)				$\eta_{2,4\text{-DCP}}$(%)	n	k	R^2
	2,4-DCP	2-CP	4-CP	Phenol				
Pd-MBfR	0.8-33.7	0-4.5	0-1.7	1.3-46.7	97.0-82.6	0.48	0.1090	0.9872
MBfR	3.6-74.1	\	6.2-45.1	\	85.5-62.0	0.52	0.0488	0.9501
Pd-film reactor	1.7-15.6	0.6-3.8	0-0.7	21.7-167.8	92.5	0.95	0.0519	0.9956

thicker Pd-biofilm compared to the PdNPs-film (~30 μm vs. ~1.75 μm), the diffusion of 2,4-DCP within the thick biofilm to reach the PdNPs surface is limited, resulting in a decrease in the reaction order.

3.3.2. *Higher nitrate loading enhanced phenol removal*

NO_3^- is a common contaminant coexisted with 2,4-DCP in water and numerous studies have demonstrated that NO_3^- is a preferred electron acceptor in hydrogen autotrophic reduction [28,32], and it can also serve as a nitrogen source for microbial metabolism. Series B investigated the impact of NO_3^- loading, with influent concentrations of 120, 220, 420, 820, and 1160 μM, respectively (Table S2).

In the Pd-MBfR (Figs. 5a and 5b), as the influent concentration of NO_3^- increased from 120 μM to 420 μM, the effluent concentrations of 2,4-DCP and 2-CP increased, while the concentrations of phenol, 2,4-DCP removal rate, and dechlorination flux decreased. Low concentrations of NO_3^- ($\leq$ 420 μM) slightly inhibited the reduction of 2,4-DCP, while higher concentrations of NO_3^- ($\geq$ 820 μM) led to an inadequate supply of electron donors, moderately impacting the reduction of 2,4-DCP. On the other hand, the effluent concentrations of NO_3^-, NO_2^-, and NH_4^+, as well as denitrification flux increased with higher influent concentrations of NO_3^-. The removal of NO_3^- remained stable at 82.8% in series B1-B3 but decreased to 65.6% in series B4-B5. The process of NO_3^- reduction includes two steps: the reduction of NO_3^- to NO_2^-, which is a relatively slow reaction, and the subsequent reduction of NO_2^- to N_2, which is a faster reaction. Only when electron donor was limited, NO_2^- accumulated in the effluent. Thus, the concentration of NO_2^- can serve as an indicator to assess the availability of electron donors [5,11]. In series B4-B5, the accumulation of NO_2^- indicates a relatively insufficient supply of electron donors (H_2) [35].

In the MBfR, low concentrations of NO_3^- ($\leq$ 220 μM) had minor impact on the reduction of 2,4-DCP, while higher concentrations of NO_3^- ($\geq$ 420 μM) inhibited the reduction of 2,4-DCP. NO_3^-concentrations of 820 μM led to an inadequate supply of electron donors, resulting in a decline in 2,4-DCP removal. Since PdNPs in the Pd-film reactor were almost incapable of reducing NO_3^-, the reduction of 2,4-DCP was not influenced by the influent NO_3^- loading.

In summary, for the Pd-MBfR to achieve overall removal of both 2,4-DCP and NO_3^-, the influent NO_3^- loading should not exceed 220 μM. The differences between the Pd-MBfR and the MBfR were attributed to the competition between NO_2^-, produced by the biological reduction of NO_3^- via denitrification, and the reduction of 2,4-DCP, which was catalyzed by PdNPs. Subsequent experiments investigating the effect of NO_2^- loading and H_2 pressure confirmed this phenomenon.

3.3.3. *Higher nitrite loading lowered the selectivity to phenol*

NO_2^- is an intermediate product in the reduction of NO_3^- and is known to be toxic, exerting inhibitory effects on dechlorinating microorganisms [2,15,20,21]. Additionally, NO_2^- reduction can be catalyzed by Pd, which competed with the reduction of 2,4-DCP. Series C investigated the influence of NO_2^- loading on 2,4-DCP removal, with influent

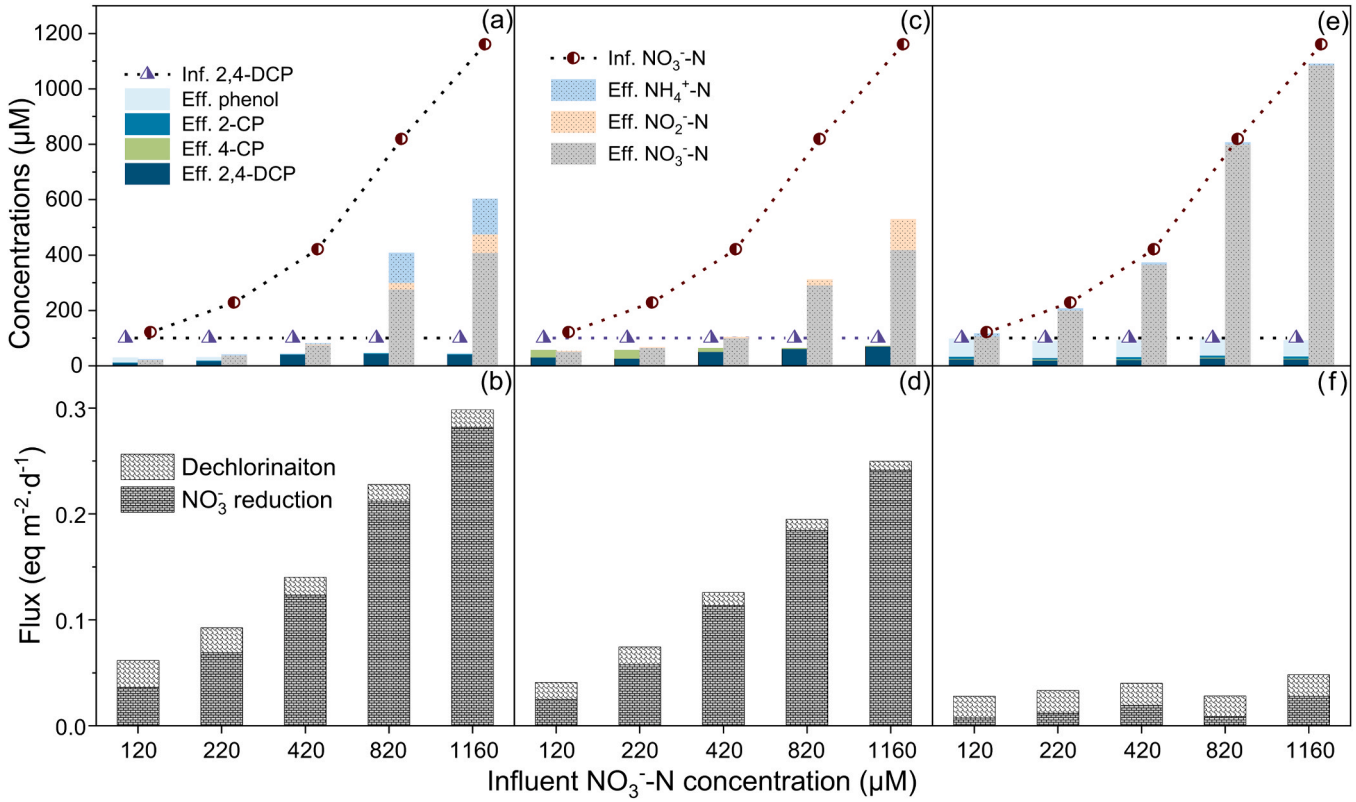

Fig. 5. The effect of influent nitrate on 2,4-dichlorophenol reduction in the Pd-biofilm reactor (a, b), the biofilm reactor (c, d), and the Pd-film reactor (e, f).

concentrations of 0, 150, 250, 550, and 750 μM, respectively (Table S2).

In the Pd-MBfR (Figs. 6a and 6b), with an increase in influent NO_2^- concentration from 0 to 150 μM, there were minimal changes in the effluent concentrations, removal rate, and dechlorination flux. As the influent NO_2^- concentration continued to rise, the removal of 2,4-DCP increased, while the concentrations of 2-CP and 4-CP initially increased and then decreased. NO_2^- inhibited the 2,4-DCP reduction, which resulted in a decrease in the removal rate of the MBfR and the Pd-film reactor. Low concentrations of NO_2^- ($\leq$ 150 μM) had minor impact on the 2,4-DCP removal, while high concentrations of NO_2^- ($\geq$ 250 μM) inhibited 2,4-DCP reduction. Increasing the influent NO_2^- loading also led to a decrease in NO_2^- removal. Among the three reactors, the inhibitory effect of NO_2^- on the reduction of 2,4-DCP followed the order of MBfR > > Pd-MBfR > Pd-film reactor. This indicates that NO_2^- had a greater impact on bioreduction of 2,4-DCP. PdNPs can rapidly catalyze NO_2^- reduction, reducing its toxicity to microorganisms and minimizing its impact on the reduction of 2,4-DCP. Considering the overall removal of 2,4-DCP and NO_2^-, the influent NO_2^- concentration should not exceed 250 μM.

3.3.4. *Accuracy control of H_2 supply accelerated dechlorination*

The effects of H_2-delivery flux on dechlorination flux and product selectivity were investigated by adjusting the H_2 pressure in the hollow-fiber membrane. In the Pd-MBfR, when the maximum H_2 flux was 60% of the total demand (3 psig H_2), 2,4-DCP removal was only 55% (Fig. 7a). Applying 6 psig H_2 resulted in the maximum H_2 flux, which stoichiometrically matched the total demand for complete dechlorination of 100 μM 2,4-DCP to phenol. Despite this, the removal was still incomplete at 68%, indicating that the actual H_2 delivery to 2,4-DCP hydrodechlorination was less than the theoretical maximum capacity. A reason is that the actual H_2 concentration at the exterior of the membrane was greater than 0, which is what gives the maximum flux. As a result, 2,4-DCP removal stepwise reached ~96% only when the H_2 pressure was increased to 15 psig (2-fold the theoretical H_2 demand), and further increases resulted in no improvement in 2,4-DCP removal.

In the MBfR, increasing the H_2 pressure promoted the reduction of both 2,4-DCP and NO_3^-. However, the impact on NO_3^- reduction was greater than that on 2,4-DCP reduction, indicating that NO_3^- was the favorable electron acceptor. In the Pd-film reactor, where there was no electron competition between 2,4-DCP and NO_3^- reduction, the removal of 2,4-DCP significantly improved with increasing H_2 pressure, reaching saturation at around 10 psig. At the same H_2 pressure, the Pd-MBfR outperformed the MBfR for 2,4-DCP reduction, but at H_2 pressures higher than 10 psig, a large amount of NH_4^+ accumulated. Therefore, it is recommended to select an optimal H_2 pressure of around 10 psig for all three reactors.

3.3.5. *pH had a significant effect on the dechlorination flux and product selectivity*

The pH plays a crucial role in microbial growth [12] and significantly influences the adsorption, dechlorination, and reduction processes of 2,4-DCP [30]. We conducted series E to investigate the pH influence by varying it at 5.0, 6.0, 7.0, 8.0, and 9.0, with applied H_2 and influent 2,4-DCP at the steady-state values of 15 psig and 100 μM, respectively (Table S2).

In the Pd-MBfR, the most effective 2,4-DCP reduction occurred at pH 7.0, and alkaline conditions had a stronger inhibitory effect on 2,4-DCP reduction compared to acidic conditions. In the MBfR, the optimum pH for 2,4-DCP reduction was 7.0, while at pH 9.0, 2,4-DCP reduction was almost negligible. Alkaline conditions had a stronger inhibitory effect on microbial reduction of 2,4-DCP. In the Pd-film reactor, the effect of pH on 2,4-DCP reduction was relatively minor, with the optimal pH range being 6.0 to 7.0. The pKa values of 2,4-DCP, 2-CP, 4-CP, and phenol are 7.80, 9.20, 8.55, and 9.89, respectively. When the pH is higher than the pKa value, chlorophenols act as weak acids and dissociate H^+, resulting in a negatively charged state [30]. Microbial cell surfaces typically possess negative charges, resulting in electrostatic repulsion between these surfaces and negatively charged chlorophenols. This repulsion can

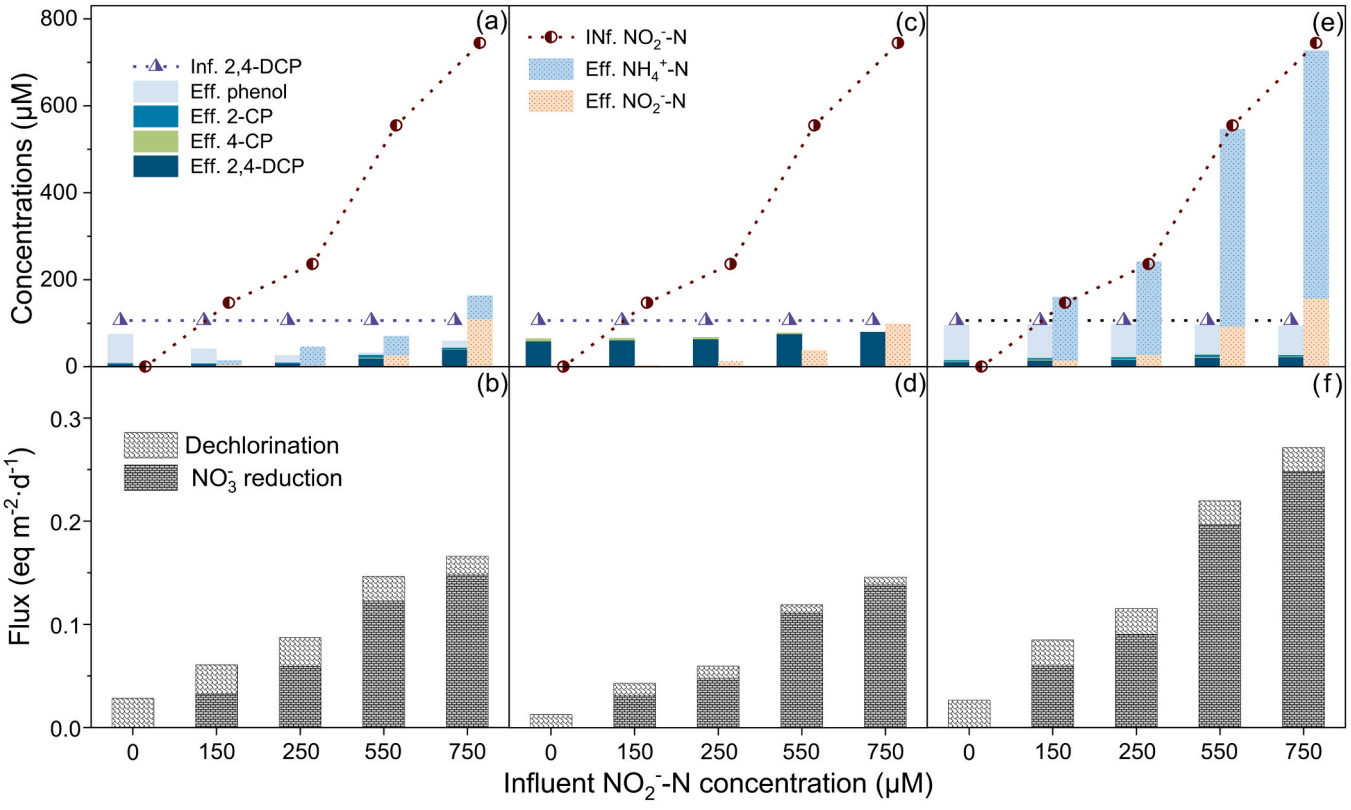

Fig. 6. The effect of influent nitrite on 2,4-dichlorophenol reduction in the Pd-biofilm reactor (a, b), the biofilm reactor (c, d), and the Pd-film reactor (e, f).

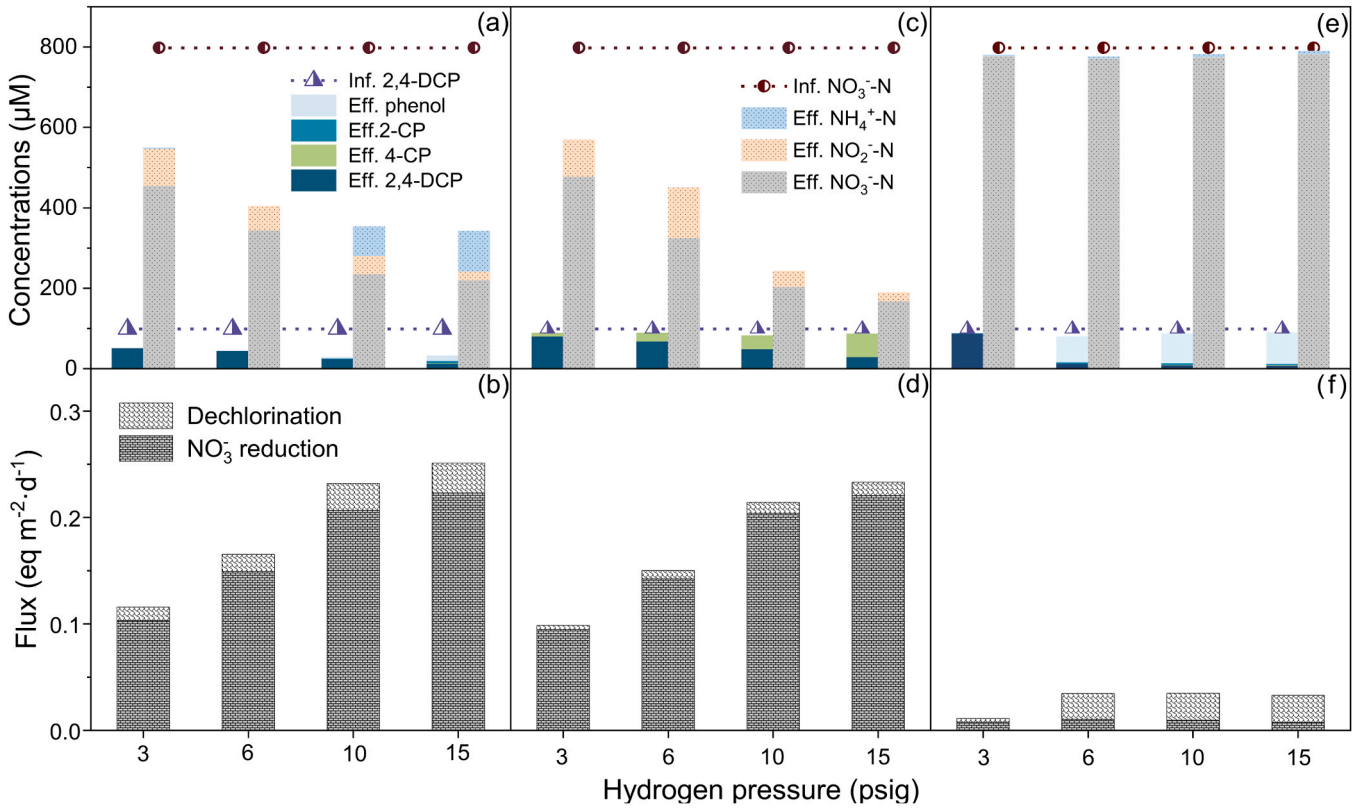

Fig. 7. The effect of hydrogen pressure on 2,4-dichlorophenol reduction in the Pd-biofilm reactor (a, b), the biofilm reactor (c, d), and the Pd-film reactor (e, f).

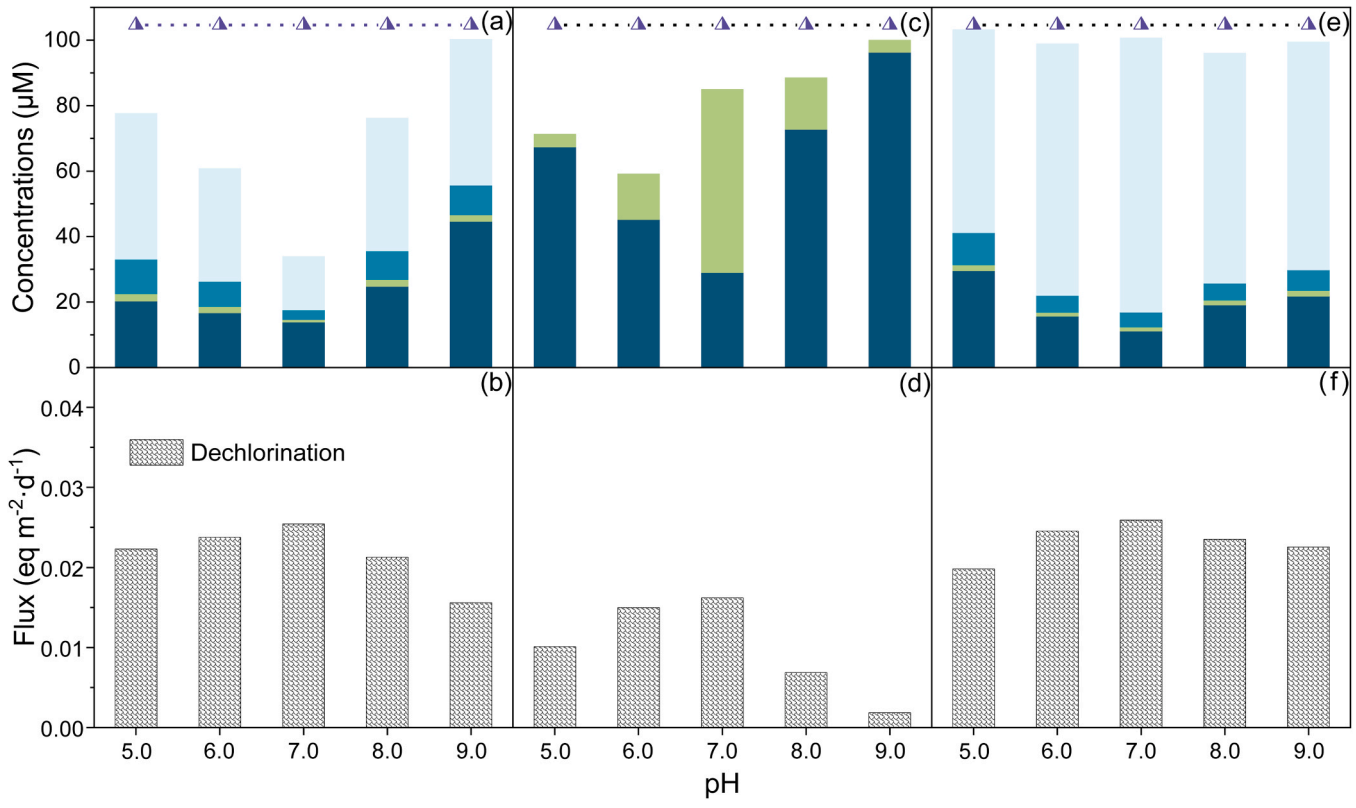

Fig. 8. The effect of pH on 2,4-dichlorophenol reduction in the Pd-biofilm reactor (a, b), the biofilm reactor (c, d), and the Pd-film reactor (e, f).

hinder the interaction of chlorophenols with the biofilm under alkaline conditions. On the other hand, excessively low pH was adverse to microbial growth and metabolism [12] and 2,4-DCP reduction. Therefore, maintaining a neutral pH range is vital to ensure effective 2,4-DCP reduction in these reactors Fig. 8.

4. Conclusion

In general, in-situ generated PdNPs associated with the biofilm to form a stable Pd-biofilm could enhance 2,4-DCP removal in the Pd-MBfR system. We investigated the effect factors on 2,4-DCP removal in the Pd-MBfR, including influent 2,4-DCP loading, NO_3^- loading, NO_2^- loading, hydrogen partial pressure, and pH. Comparative tests were also carried out using the biotic MBfR and the abiotic Pd-film reactor contain PdNPs alone in parallel, and the major summary points are as follows:

(1) Compared to sole biofilm and PdNPs, coupling of PdNPs with biofilm improved the removal of 2,4-DCP and total phenols. The Pd-MBfR showed optimal 2,4-DCP removal rate (96%) for effluent concentrations below 70 μM.

(2) In the Pd-MBfR and the MBfR, there was competition between NO_3^- reduction and 2,4-DCP reduction, and NO_3^- reduction was preferred. The reduction of 2,4-DCP would be suppressed when the influent NO_3^- concentration exceed 220 μM.

(3) NO_2^- inhibited 2,4-DCP reduction in all three reactors, but the inhibitory effect on bioreduction of 2,4-DCP is greater than on Pd-catalyzed reduction. When electron donors were sufficient, PdNPs rapidly catalyzed NO_2^- reduction, reducing the impact of NO_2^- on 2,4-DCP reduction.

(4) Increasing hydrogen pressure promoted the reduction of 2,4-DCP and NO_3^- in the Pd-MBfR. While at higher hydrogen pressure (15 psig), the reduction of 2,4-DCP was promoted, but excessive NO_3^- reduction led to the accumulation of NH_4^+. When NO_3^- was present, the hydrogen partial pressure should not exceed 10 psig.

(5) In the Pd-MBfR and the MBfR, the optimal pH was 7.0 and 6.0, respectively, with alkaline conditions exhibiting a stronger inhibition on 2,4-DCP reduction compared to acidic conditions. In the Pd-film reactor, the pH had a relatively small effect on 2,4-DCP reduction, with the optimal pH range being 6.0 to 7.0.

CRediT authorship contribution statement

Lichtfouse Eric: Supervision, Writing – review & editing. **Li Xiaodi:** Writing – review & editing. **Yang Lin:** Writing – review & editing. **Pang Si:** Conceptualization, Methodology, Writing – review & editing. **Liu Hongbo:** Funding acquisition, Project administration, Supervision, Validation, Writing – review & editing. **Xia Siqing:** Methodology, Supervision, Writing – review & editing. **Wu Chengyang:** Conceptualization, Formal analysis, Investigation, Methodology, Resources, Visualization, Writing – original draft, Writing – review & editing, Data curation. **Zhou Jingzhou:** Data curation, Formal analysis, Investigation, Validation, Writing – original draft.

Declaration of Competing Interest

The authors declare that they have no known competing financial interests or personal relationships that could have appeared to influence the work reported in this paper.

Data Availability

Data will be made available on request.

Acknowledgements

The authors would like to acknowledge the co-funding of this work by the Natural Science Foundation of Shanghai (No.22ZR1443200) and the National Natural Science Foundation of China (No.52070130).

Appendix A. Supporting information

Supplementary data associated with this article can be found in the online version at doi:10.1016/j.jece.2024.112176.

References

[1] E.J. Bedmar, E.F. Robles, M.J. Delgado, The complete denitrification pathway of the symbiotic, nitrogen-fixing bacterium Bradyrhizobium japonicum, Biochem. Soc. Trans. 33 (2005) 141–144.
[2] E. Bruce, P.L.M. Rittmann, Environmental Biotechnology: Principles and Applications, McGraw-Hill Book Co, New York, 2020.
[3] J. Chung, R. Nerenberg, B.E. Rittmann, Bio-reduction of soluble chromate using a hydrogen-based membrane biofilm reactor, Water Res. 40 (8) (2006) 1634–1642.
[4] J. Chung, R. Nerenberg, B.E. Rittmann, Bioreduction of selenate using a hydrogen-based membrane biofilm reactor, Environ. Sci. Technol. 40 (5) (2006) 1664–1671.
[5] J. Chung, B.E. Rittmann, W.F. Wright, R.H. Bowman, Simultaneous bio-reduction of nitrate, perchlorate, selenate, chromate, arsenate, and dibromochloropropane using a hydrogen-based membrane biofilm reactor, Biodegradation 18 (2) (2007) 199–209.
[6] J.D. Coates, R. Chakraborty, J.G. Lack, S.M. O'Connor, K.A. Cole, K.S. Bender, L. A. Achenbach, Anaerobic benzene oxidation coupled to nitrate reduction in pure culture by two strains of Dechloromonas, Nature 411 (6841) (2001) 1039–1043.
[7] J.D. Coates, R. Chakraborty, M.J. McInerney, Anaerobic benzene biodegradation - a new era, Res. Microbiol. 153 (10) (2002) 621–628.
[8] L. Ding, H. Zhou, S. Li, X. Lan, X. Chen, S. Zeng, Boosting visible photocatalytic degradation of 2,4-dichlorophenol and phenol efficiency by stable core@shell hybrid Ag3PO4@polypyrrole, Colloids Surf. A: Physicochem. Eng. Asp. 648 (2022) 129296.
[9] Z.N. Garba, W. Zhou, I. Lawan, W. Xiao, M. Zhang, L. Wang, L. Chen, Z. Yuan, An overview of chlorophenols as contaminants and their removal from wastewater by adsorption: a review, J. Environ. Manag. 241 (2019) 59–75.
[10] M. Gonzalez, K.S.B. Miglioranza, V.M. Shimabukuro, O.M. Quiroz Londono, D. E. Martinez, J.E. Aizpún, V.J. Moreno, Surface and groundwater pollution by organochlorine compounds in a typical soybean system from the south Pampa, Argentina, Environ. Earth Sci. 65 (2) (2012) 481–491.
[11] K.C. Lee, B.E. Rittmann, A novel hollow-fiber membrane biofilm reactor for autohydrogenotrophic denitrification of drinking water, Water Sci. Technol. 41 (4-5) (2000) 219–226.
[12] K.C. Lee, B.E. Rittmann, Effects of pH and precipitation on autohydrogenotrophic denitrification using the hollow-fiber membrane-biofilm reactor, Water Res. 37 (7) (2003) 1551–1556.
[13] Z. Liu, C. Zhou, A. Ontiveros-Valencia, Y.-H. Luo, M. Long, H. Xu, B.E. Rittmann, Accurate O2 delivery enabled benzene biodegradation through aerobic activation followed by denitrification-coupled mineralization, Biotechnol. Bioeng. 115 (8) (2018) 1988–1999.
[14] M. Long, C. Zeng, Z. Wang, S. Xia, C. Zhou, Complete dechlorination and mineralization of para-chlorophenol (4-CP) in a hydrogen-based membrane biofilm reactor (MBfR), J. Clean. Prod. 276 (2020) 123257.
[15] Yu-Ran Luo, Comprehensive Handbook of Chemical Bond Energies, CRC Press: Boca Raton, FL, 2007.
[16] Y.-H. Luo, C. Zhou, Y. Bi, X. Long, B. Wang, Y. Tang, R. Krajmalnik-Brown, B. E. Rittmann, Long-term continuous co-reduction of 1,1,1-trichloroethane and trichloroethene over palladium nanoparticles spontaneously deposited on H2-transfer membranes, Environ. Sci. Technol. 55 (3) (2021) 2057–2066.
[17] O. Modin, K. Fukushi, K. Yamamoto, Denitrification with methane as external carbon source, Water Res. 41 (12) (2007) 2726–2738.
[18] M.R. Samarghandi, A. Dargahi, A. Rahmani, A. Shabanloo, A. Ansari, D. Nematollahi, Application of a fluidized three-dimensional electrochemical reactor with Ti/SnO2–Sb/β-PbO2 anode and granular activated carbon particles for degradation and mineralization of 2,4-dichlorophenol: Process optimization and degradation pathway, Chemosphere 279 (2021) 130640.
[19] Y. Tang, C. Zhou, S.W. Van Ginkel, A. Ontiveros-Valencia, J. Shin, B.E. Rittmann, Hydrogen permeability of the hollow fibers used in H2-based membrane biofilm reactors, J. Membr. Sci. 407-408 (2012) 176–183.
[20] D.O. Tas, S.G. Pavlostathis, Effect of nitrate reduction on the microbial reductive transformation of pentachloronitrobenzene, Environ. Sci. Technol. 42 (9) (2008) 3234–3240.
[21] United States Environmental Protection Agency, 2012. Drinking Water Standards and Health Advisories. Office of Water, U.S. EPA, Washington, D.C. EPA 822-B-00–001.
[22] Y. Wang, L. Wang, Y. Zhang, X. Mao, W. Tan, Y. Zhang, X. Wang, M. Chang, R. Guo, B. Xi, Perdisulfate-assisted advanced oxidation of 2,4-dichlorophenol by bio-inspired iron encapsulated biochar catalyst, J. Colloid Interface Sci. 592 (2021) 358–370.
[23] W. Wei, H. Deng, G. Li, C. Gong, J. Lu, Screening and culture condition of a Type II methanotroph, Chin. J. Appl. Environ. Biol. 21 (3) (2015) 455–463.
[24] C. Wu, L. Zhou, C. Zhou, Y. Zhou, S. Xia, B.E. Rittmann, Co-removal of 2,4-dichlorophenol and nitrate using a palladized biofilm: denitrification-promoted microbial mineralization following catalytic dechlorination, J. Hazard. Mater. 422 (2022) 126916.

[25] C. Wu, L. Zhou, C. Zhou, Y. Zhou, J. Zhou, S. Xia, B.E. Rittmann, A kinetic model for 2,4-dichlorophenol adsorption and hydrodechlorination over a palladized biofilm, Water Res. 214 (2022) 118201.
[26] C. Wu, L. Zhou, Y. Zhou, C. Zhou, S. Xia, B.E. Rittmann, Dechlorination of 2,4-dichlorophenol in a hydrogen-based membrane palladium-film reactor: Performance, mechanisms, and model development, Water Res. 188 (2021) 116465.
[27] C. Wu, J. Zhou, S. Pang, L. Yang, E. Lichtfouse, H. Liu, S. Xia, B.E. Rittmann, Reduction and precipitation of chromium(VI) using a palladized membrane biofilm reactor, Water Res. 249 (2024) 120878.
[28] S. Xia, J. Liang, X. Xu, S. Shen, Simultaneous removal of selected oxidized contaminants in groundwater using a continuously stirred hydrogen-based membrane biofilm reactor, J. Environ. Sci. 25 (1) (2013) 96–104.
[29] S. Xia, X. Xu, C. Zhou, C. Wang, L. Zhou, B.E. Rittmann, Direct delivery of CO_2 into a hydrogen-based membrane biofilm reactor and model development, Chem. Eng. J. 290 (2016) 154–160.
[30] J. Xu, L. Tan, S.A. Baig, D. Wu, X. Lv, X. Xu, Dechlorination of 2,4-dichlorophenol by nanoscale magnetic Pd/Fe particles: Effects of pH, temperature, common dissolved ions and humic acid, Chem. Eng. J. 231 (2013) 26–35.
[31] K. Yang, Y. Zhao, M. Ji, Z. Li, S. Zhai, X. Zhou, Q. Wang, C. Wang, B. Liang, Challenges and opportunities for the biodegradation of chlorophenols: aerobic, anaerobic and bioelectrochemical processes, Water Res. 193 (2021) 116862.
[32] H.-P. Zhao, Z.E. Ilhan, A. Ontiveros-Valencia, Y. Tang, B.E. Rittmann, R. Krajmalnik-Brown, Effects of multiple electron acceptors on microbial interactions in a hydrogen-based biofilm, Environ. Sci. Technol. 47 (13) (2013) 7396–7403.
[33] T. Zhao, H.E. C, L. Zhang, X. Quan, Y. Zhao, Kinetics of affinity to methane oxidation by Chryseobacterium sp.from aged-refuse, J. Chem. Ind. Eng. (China) 62 (7) (2011) 1915–1921.
[34] C. Zhou, Z. Wang, A.K. Marcus, B.E. Rittmann, Biofilm-enhanced continuous synthesis and stabilization of palladium nanoparticles (PdNPs), Environ. Sci.: Nano 3 (6) (2016) 1396–1404.
[35] M.C. Ziv-El, B.E. Rittmann, Systematic evaluation of nitrate and perchlorate bioreduction kinetics in groundwater using a hydrogen-based membrane biofilm reactor, Water Res. 43 (1) (2009) 173–181.

Enhanced removal of 2,4-dichlorophenol by coupling of Pd nanoparticles with biofilm

Chengyang Wu [a], Jingzhou Zhou [b], Si Pang [b], Lin Yang [b], Xiaodi Li [b], Eric Lichtfouse [c], Siqing Xia [b], Hongbo Liu [a, *]

[a] *School of Environment and Architecture, University of Shanghai for Science and Technology, 516 Jungong Road, Shanghai, China*

[b] *State Key Laboratory of Pollution Control and Resource Reuse, College of Environmental Science and Engineering, Tongji University, 1239 Siping Road, Shanghai, China*

c State Key Laboratory of Multiphase Flow in Power Engineering, Xi'an Jiaotong University,28 Xianning West Rd, Xi'an, Shaanxi, 710049 P.R. China.

* Corresponding author

E-mail address: Liuhb@usst.edu.cn (H. Liu)

Summary:

Pages: 6

Figures: 3

Tables: 2

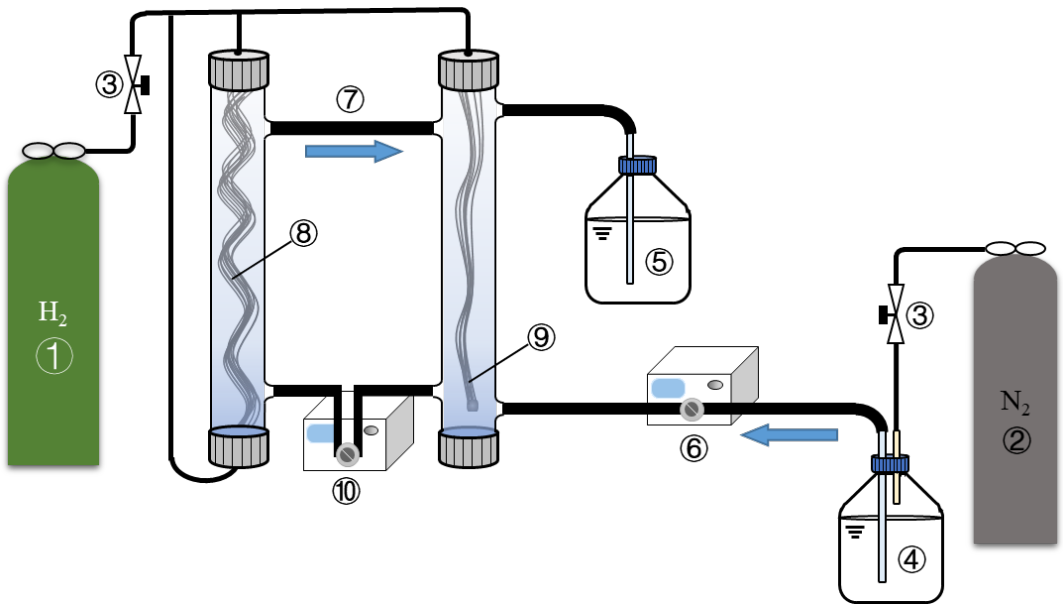

Figure S1. Schematic of the Pd-MBfR system: ① pure-H_2 gas tank to feed the fiber bundles; ② pure-N_2 gas to feed the headspace of the influent medium bottle; ③ gas-pressure regulator; ④ influent-medium bottle; ⑤ effluent bottle; ⑥ influent pump; ⑦ Recirculation configuration (the blue arrow indicates the flow direction); ⑧ main bundle with 32 fibers; ⑨ sampling coupon bundle with 10 fibers; and ⑩ recirculation pump.

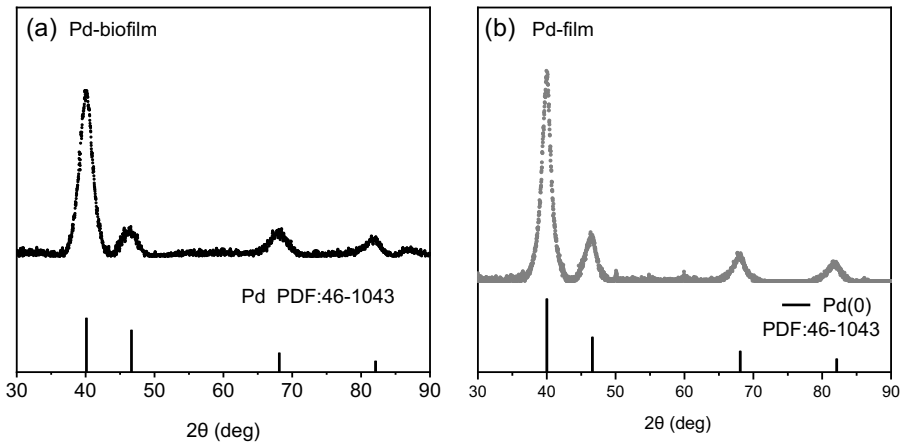

Figure S2. XRD spectra of the solid powders collected from Pd-biofilm (a) and Pd0- film (b).

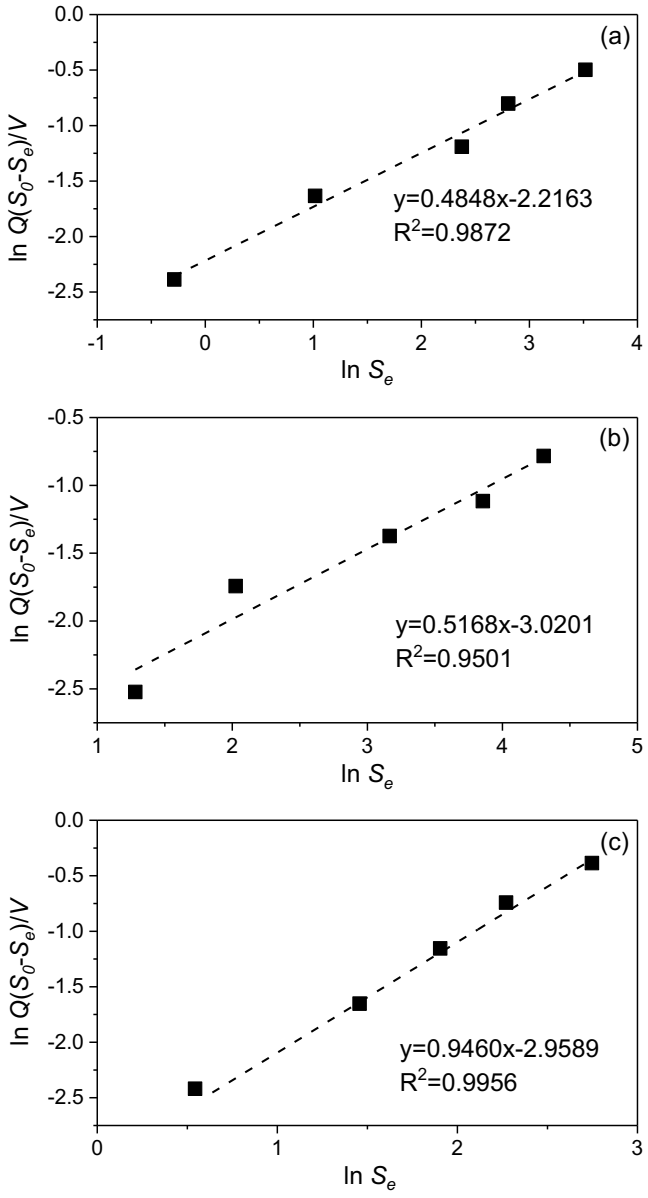

Figure S3. Reaction kinetics parameters of 2,4-DCP under different influent concentrations in Pd-MBfR (a), MBfR (b), and MPfR (c).

Process of raw sequences in microbial community analyses

We removed sequences shorter than 200 bps, homopolymers of more than 6 bps, and primer mismatches, or a quality score lower than 25. Chimeric sequences were removed by HCHIME and then the operational taxonomic unit (OTUs) was clustered with 97% similarity cutoff using UPARSE (version 7.0.1). Representative sequences were aligned to the silva (SSU138) 16S rRNA database by RDP Classifier (version 2.11), using confidence threshold of 0.7.

Table S1. Composition of the mineral-salts medium fed to the reactors.

Component	Concentration ($mg \cdot L^{-1}$)	Contents	Concentration ($mg \cdot L^{-1}$)
$NaHCO_3$ *	50	$ZnCl_2$	0.070
KH_2PO_4	20	$Na_2MoO_4 \cdot 2H_2O$	0.036
$MgCl_2 \cdot 6H_2O$	2.0	$NiCl_2 \cdot 6H_2O$	0.024
$FeCl_2 \cdot 4H_2O$	0.10	Na_2SeO_3	0.009
$CaCl_2 \cdot 2H_2O$	0.10	$Na_2WO_4 \cdot 2H_2O$	0.008
$CoCl_2 \cdot 6H_2O$	0.19	H_3BO_3	0.006
$MnCl_2 \cdot 4H_2O$	0.10	$CuCl_2 \cdot 2H_2O$	0.002

Table S2. Variable system conditions for the short-term experiments.

Series	Influent concentration (μM)			H_2 pressure (psig)	Influent pH
	2,4-DCP	NO_3^-	NO_2^-		
Steady state	100	85	0	15	7.0
A1	25				
A2	45				
A3	70	85	0	15	7.0
A4	100				
A5	140				
B1		120			
B2		220			
B3	100	420	0	15	7.0
B4		820			
B5		1160			
C1			0		
C2			150		
C3	100	85	250	15	7.0
C4			550		
C5			750		
D1				3	
D2	100	820	0	6	7.0
D3				10	
D4				15	
E1					5.0
E2					6.0
E3	100	85	0	15	7.0
E4					8.0
E5					9.0